Simulation of a MEMS Coriolis Gyroscope with Closed-Loop Control for Arbitrary Inertial Force, Angular Rate, and Quadrature Inputs

Charles H. Tally, Richard L. Waters*, Paul D. Swanson
*Senior Member IEEE
Advanced Integrated Circuits Technology Code 55250
SSC Pacific
San Diego, CA/USA
charles.tally@navy.mil

***Abstract*—A closed-loop control system for a MEMS gyroscope is proposed which greatly restricts the mechanical freedom of the sense mass while accurately measuring the total external force acting upon the sense mass. This is realized by an algorithm which uses the previous three sense mass position measurements to generate a position-, velocity-, and acceleration-dependant feedback force on the sense mass. The feedback force is equal and opposite to the average total external force the sense mass was subject to during the previous three position samples. As the feedback sampling rate increases, so too does the control loop's ability to both spatially confine the sense mass and determine the total external force acting on the sense mass. For a 1.05 MHz feedback sampling rate, we achieve a measurement of the external force with less than 5 parts per million error, and constrain the sense mass to displacements of less than 10nm.**

I. Background and Introduction

A typical two-mass MEMS Coriolis gyroscope consists of two silicon masses with independent silicon suspensions: a drive mass with springs designed to deflect primarily in the drive-mode direction (x_d) and a sense mass with a suspension designed to deflect primarily in an orthogonal sense-mode direction (x_s) [1]. The drive mass is actuated harmonically on resonance giving it a non-zero velocity along the drive-axis. The sense mass is then subject to: Coriolis forces induced by external rotations oriented about the axis perpendicular to both the drive- and sense-mode axes; Quadrature forces induced by undesired drive/sense mode mechanical coupling resulting from imperfect silicon spring fabrication; and inertial forces acting along the sense- axis.

The system's dynamics can be modeled by a coupled set of damped oscillator equations. The drive mode oscillator is characterized by the drive mass (m_d), drive-mode quality factor (Q_d) and mechanical resonant frequency (ω_d). Similarly, the sense-mode oscillator is characterized by the sense-mass (m_s), sense-mode quality factor (Q_s) and mechanical resonant frequency (ω_s). The gyroscope's dynamics are then modeled by a set of differential equations:

$$\frac{d^2x_d}{dt^2}+\frac{\omega_d}{Q_d}\frac{dx_d}{dt}+\omega_d^2x_d=\frac{F_d\sin(\omega_d t)}{m_d}, \quad (1)$$

$$\frac{d^2x_s}{dt^2}+\frac{\omega_s}{Q_s}\frac{dx_s}{dt}+\omega_s^2x_s=\frac{F_C(t)+F_Q(t)+F_I(t)+F_{FB}(t)}{m_s}. \quad (2)$$

The drive mode oscillator is driven by a sinusoidal force of constant amplitude (F_d) at the drive frequency (ω_d). The sense mode oscillator is driven by time-varying inertial forces, $F_I(t)$, and Quadrature and Coriolis forces given by

$$F_Q(t)=-k_{xy}x_d, \quad (3)$$

$$F_C(t)=-2m_dv_d\Omega(t), \quad (4)$$

where k_{xy} is the mechanical coupling parameter determined by the level of imperfection in silicon spring fabrication, $v_d=dx_d/dt$ is the drive mode velocity, and $\Omega(t)$ is the time-varying external rotation rate of the device oriented about the axis perpendicular to both the drive- and sense-mode axes.

The final force acting on the sense mode oscillator, $F_{FB}(t)$, is the feedback force generated by the closed-loop control system outlined herein. The correct choice of feedback force algorithm allows for accurate determination of the total external force acting on the sense mass:

$$F_E(t)=F_C(t)+F_Q(t)+F_I(t). \quad (5)$$

Additionally, the feedback force must restrict the sense mass to near-zero displacements, so that the transducer responsible

for measuring the position of the sense mass has a highly linear output over the device's entire operational range.

II. Evolving the Equations of Motion

To solve equations (1) and (2) numerically, we first consider the general numerical method of evolving the equation of motion for a damped oscillator under the influence of an arbitrary, time-dependant force, $F(t)$. For a damped oscillator of a given mass (m), quality factor (Q) and resonant frequency (ω), we rewrite the equation of motion in terms of the mass' acceleration:

$$a(t) = \frac{d^2x(t)}{dt^2} = \frac{F(t)}{m} - \frac{\omega}{Q}\frac{dx(t)}{dt} - \omega^2 x(t). \qquad (6)$$

where $x(t)$ is the position of the mass in time. We can then write the time-discretized form of (6) as

$$a_i = \frac{F_i}{m} - \frac{\omega}{Q} v_i - \omega^2 x_i, \qquad (7)$$

Where i is an integer that determines the current time: $t_i = i \cdot \Delta t$, and Δt is the numerical integration time step.

Given the initial conditions: F_0, x_0, and v_0 at t_0, the initial acceleration (a_0) can be calculated. To determine the mass' position at the next point in time, we employ the Feynman-Newton method [2] of discrete time evolution:

$$v_{i+1/2} = v_i + a_i \cdot \frac{\Delta t}{2}, \qquad (8)$$

$$x_{i+1} = x_i + v_{i+1/2} \cdot \Delta t, \qquad (9)$$

$$v_{i+1} = v_i + a_i \cdot \Delta t. \qquad (10)$$

To calculate the new position x_{i+1}, this method uses the velocity value at the midpoint in time between t_i and t_{i+1}. With equations (9) and (10), the new acceleration a_{i+1} can be calculated using (7) — so long as the total force acting on the mass (F_i) is known at each time step.

In the case of the drive mode oscillator (1), the driving force is user generated, sinusoidal, and well defined at all time steps. Thus, the drive mode position and velocity ($x_{d,i}$ and $v_{d,i}$) can be adequately determined by substituting m_d, Q_d, and ω_d into (7) and repeatedly employing (8)-(10).

For the sense mode oscillator (2), the same approach can be used by substituting m_s, Q_s, and ω_s into (7), however, the total driving force is more complicated. Plugging discretized versions of (2)-(3) into (5) gives

$$F_{E,i} = -2m_d v_{d,i} \cdot \Omega_i - k_{xy} \cdot x_{d,i} + F_{I,i}. \qquad (11)$$

where $x_{d,i}$ and $v_{d,i}$ are the calculated position and velocity of the drive mass. The drive mass, m_d, and the Quadrature coupling term, k_{xy}, are time-independent system parameters. In real world scenarios, the external rotation rate, Ω_i and the sense-axis inertial force, $F_{I,i}$, are time-dependant unknown parameters to be solved for.

In this simulation, Ω_i and $F_{I,i}$ are provided by the user as analytical equations or as test data. In doing so, however, there is no loss of generality. As will be shown in the next section, the feedback control algorithm accurately measures the total external force (11) without any knowledge of the user-provided force/rotation information. Thus, even in the presence of (unknown) real-world forces, the control algorithm accurately determines the total external force.

III. The Feedback Control Algorithm

The closed-loop control algorithm is responsible for generating the feedback force term in (2), $F_{FB}(t)$. The applied feedback force must constrain the sense mass to move only within the linear range of the transducer responsible for measuring the position of the sense mass. Additionally, the control loop must accurately measure the total external force acting on the sense mass.

The control algorithm uses the transducer output data stream to determine the sense mass' position at each sampling time ($x_{s,i}$). The algorithm then uses this data to generate a feedback force with components proportional to the sense mass' position, velocity, and acceleration. The velocity and acceleration of the sense mass at t_i is given by:

$$v_{s,i} \cong \frac{x_{s,i+1} + x_{s,i-1}}{(2 \cdot \Delta t)}, \qquad (12)$$

$$a_{s,i} \cong \frac{x_{s,i+1} - 2 \cdot x_{s,i} + x_{s,i-1}}{(\Delta t)^2}. \qquad (13)$$

After three consecutive sense mass position measurements are made, a feedback force is applied to the sense mass at the next (fourth) time step. The feedback force is given by

$$F_{FBi} \cong F_{FBi-1} - (\alpha \cdot a_{s,i-2} + \beta \cdot v_{s,i-2} + \gamma \cdot x_{s,i-2}). \qquad (14)$$

where α, β, and γ are user-controlled parameters. For the choice of $F_{FB0} = 0$, the feedback force, (14), can be written

$$F_{FBi} \cong -\left(\alpha \cdot \sum_{j=1}^{i-2} a_{s,j} + \beta \cdot \sum_{j=1}^{i-2} v_{s,j} + \gamma \cdot \sum_{j=1}^{i-2} x_{s,j} \right). \qquad (15)$$

By starting with the discretized form of (2), and substituting (15) for F_{FBi}, the total external force can be written:

$$F_{E_i} \cong +\left(m_s \cdot \sum_{j=1}^{i} a_{s,j} + \frac{\omega_s}{Q_s} \cdot \sum_{j=1}^{i} v_{s,j} + m_s \omega_s^2 \cdot \sum_{j=1}^{i} x_{s,j} \right) . \quad (16)$$

Comparing equations (15)-(16), we find that if we choose $\alpha = m_s$, $\beta = \omega_s / Q_s$ and $\gamma = m_s \omega^2$ in (15), then the feedback force applied at t_{i+2} is equal and opposite to the total external force that existed t_i. The measured value of the external force is thus

$$F_{E_i} = -F_{FB_{i+2}} . \quad (17)$$

Equation (17) shows that if we can accurately measure the feedback force exerted on the sense mass by the control loop, we also determine the external force acting on the sense mass with a two sample delay.

Once the total external force is obtained, the external rotational rate $\Omega(t)$ must be determined. First, inertial forces can be removed from the total external force signal via high pass filtering, since Quadrature and Coriolis forces occur at the drive mass mechanical resonant frequency near 10kHz. Coriolis and Quadrature forces are intrinsically $\pi/2$ out of phase, allowing use of synchronous demodulation to isolate the Coriolis force. Amplitude demodulation and subsequent rate table characterization can be used to correlate the filtered data signal to an external rotation rate.

IV. Simulation Details

Included herein are simulation parameters for a system in which a MEMS gyroscope is subject to a variety of external time varying inertial forces and rotations. The simulation evolves the drive and sense mode oscillator equations of motion for four seconds of real-world time.

The drive mode oscillator ($m_d = 10^{-5}\,\text{kg}$, $Q_d = 1000$, $f_d = 9.5\text{kHz}$) is driven on resonance by a sinusoidal force of amplitude $F_d = 4.15 \times 10^{-5}\,\text{N}$, generating stable oscillations of amplitude $x_d = 11.6\mu\text{m}$ at steady state. The sense mode oscillator ($m_s = 1.5 \times 10^{-6}\,\text{kg}$, $Q_s = 1000$, $f_s = 10\text{kHz}$) is subsequently driven by time-dependant Quadrature, Coriolis and inertial forces defined by the user.

The strength of the Quadrature force is defined by k_{xy}. In this simulation, $k_{xy} = k_s / 100$, where k_s is the mechanical spring constant of the sense mode oscillator ($k_s = m_s \omega_s^2$). This Quadrature strength is consistent with the typical imperfections in Silicon springs resultant from current DRIE fabrication methods [3].

Coriolis forces are exerted upon the sense mass when external rotations are present. In this simulation the Coriolis force is driven by a time-dependant rotational rate of the form

$$\Omega(t) = \Omega_0 + \Omega_1 \cdot e^{-2\left(\frac{t-t_1}{\tau_\Omega}\right)^2} + \Omega_2 \cdot e^{-2\left(\frac{t-t_2}{\tau_\Omega}\right)^2} , \quad (18)$$

where $\Omega_0 = \pi/4\,(\text{rad/s})$, $\Omega_1 = -2\pi\,(\text{rad/s})$, $\Omega_2 = 3\pi\,(\text{rad/s})$, $t_1 = 2.0\ (\text{s})$, $t_2 = 3.0\ (\text{s})$, and $\tau_\Omega = 1.0\ (\text{s})$.

The sense mass is also subject to a time-dependant inertial force of the form

$$F_I(t) = F_0 + F_1 \cdot e^{-2\left(\frac{t-t_1}{\tau_I}\right)^2} + F_2 \sin(\omega_I t) \quad (19)$$

where $F_0 = -m_s g\ (\text{N})$, $F_1 = 2 m_s g\ (\text{N})$, $F_2 = m_s g / 2\ (\text{N})$, $t_1 = 2.5\ (\text{s})$, $\tau_I = 0.4\ (\text{s})$, $\omega_I = 500\ (\text{Hz})$, and $g = 9.8\,(\text{m/s}^2)$.

The Coriolis and Quadrature forces both act at the drive mode resonant frequency of 9.5kHz, while DC and other lower-frequency content exists in the components of (18)-(19). A variety of relatively strong, rapidly changing inputs were chosen to demonstrate the control loop's ability to remain stable, and accurately measure the total external force, even in highly dynamic environments.

V. Results

Figure 1 shows the actual total external force with the calculated total external force data overlaid over a short time period. It can be seen qualitatively that our method of force feedback is very successful in reproducing the form of the total external force incident upon the sense mass. To quantify the accuracy of our measurements, however, we need to consider the relative error of our force measurements.

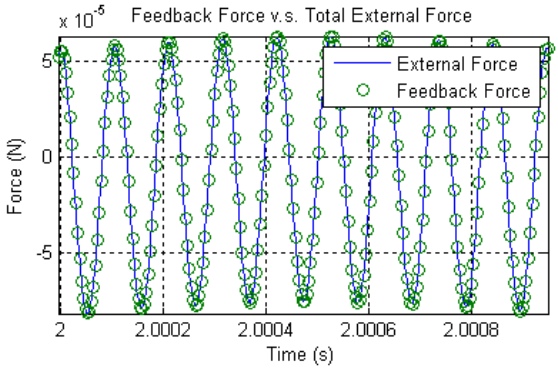

Figure 1. The actual total external force is shown with the feedback loop's estimate of the total external force overlaid. The choice of feedback force, (14), allows for very accurate estimation of the actual external force via (17).

The relative error of the control loop at a given time, t_i, is defined as the difference between the measured external force and the actual external force, divided by the actual external force. Using (17) the relative error can be calculated as

$$\varepsilon_i = \frac{-F_{FB_{i+2}} - F_{E_i}}{F_{E_i}} . \quad (20)$$

The feedback force is calculated using (14) and carries an intrinsic two sample time delay. Thus, to avoid timing errors when calculating the relative error, we compare the feedback force generated at t_{i+2} with the actual external force which existed at t_i. Figure two shows the absolute value of the relative error calculated at each forcing cycle over the entire 4 second simulation. The time-averaged relative error has a magnitude of 4.62×10^{-6} — less than five parts per million.

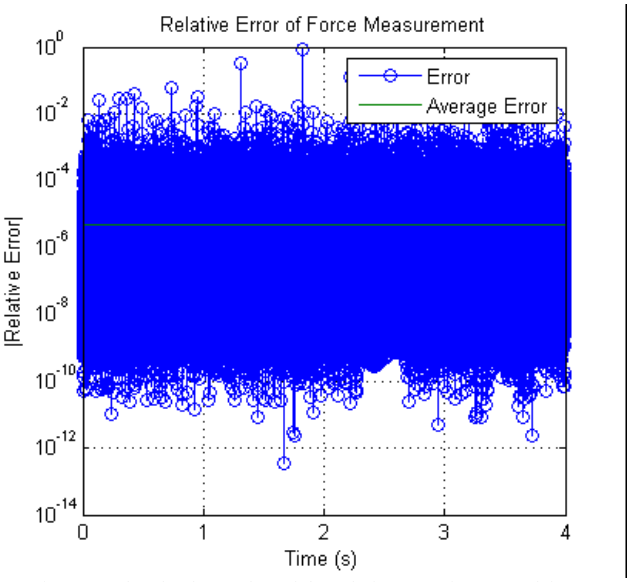

Figure 2. The absolute value of the relative error in external force measurements, (20), is plotted vs. time. The average value of 4.62×10^{-6} is overlaid – showing that a better than 5 ppm error is achieved.

In addition to accurately determining the external force on the sense mass, a successful loop closure needs to constrain the sense mass to near zero displacements. This ensures that the output of the position measurement transducer remains linear over the life of the device. Additionally, the scale factor of the device remains accurate regardless of the magnitude of the external force, so long as the feedback controller can physically produce an equal and opposite force.

Figure 3 shows the sense mass position during the simulation. The mass displacement grows until a steady state is reached. The control algorithm holds the peak amplitude of sense mass oscillations nearly constant, despite changes in input forces and rotations. The faster the forcer control loop sampling rate, the tighter the sense mass can be constrained. In our simulation, the forcer sampling rate was set to 1.05MHz, which allowed us to limit sense mass motion to less than 8.5nm displacements — well within the linear range of most optical and capacitive transducers.

Figure 4 shows that the peak amplitude of the sense mass displacements decreases inversely as the feedback sampling rate increases. The x-axis is plotted as the ratio of the force sampling rate to the mechanical resonant frequency of the sense mass oscillator. As the force sampling approaches the oscillator's mechanical resonance, the ability of the forcing loop to hold the proof mass centered reduces dramatically.

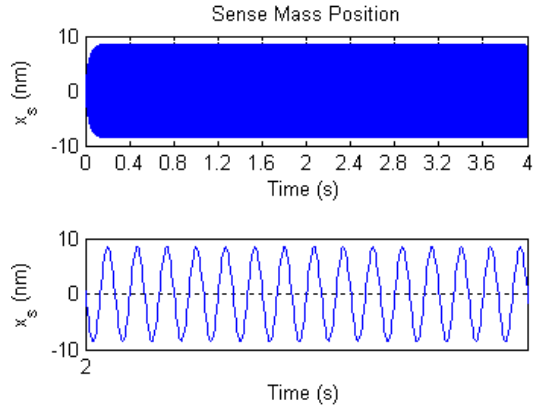

Figure 3. The sense mass position as a function of time on long (top) and short (bottom) time scales. In the top image, the 9.5-10kHz oscillations of the sense mass manifest themselves as an envelope over the long time interval.

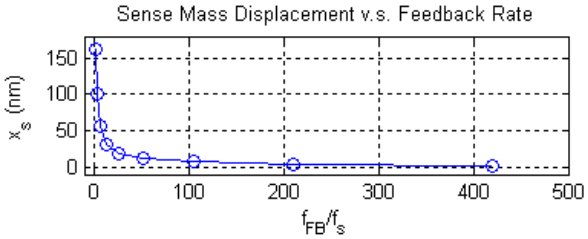

Figure 4. Peak sense mass displacement vs. feedback sampling rate (normalized to the sense mass resonant frequency). As the sampling rate increases the sense mass displacements tend to zero. As the force feedback rate approaches the mechanical resonant frequency, the displacements grow.

VI. Future Work

In the future, this simulation will process the calculated external force signal data (e.g. low pass filtering, synchronous demodulation, amplitude demodulation) to determine the external rotation rate $\Omega(t)$. Additionally, a second control loop will be implemented to ensure the drive mass oscillator is actuated at constant amplitude, and always at the drive mode resonance, even in the incident of perturbing forces. Lastly, this algorithm will be incorporated into the control electronics of a patent pending two-mass MEMS Coriolis gyroscope design which is currently in fabrication.

References

[1] Y. Mochida, M. Tamura,, and K. Ohwada, "A Micromachined Vibrating Rate Gyroscope with Independent Beams for the Drive and Detection Modes", Micro Electro Mechanical Systems, 1999. MEMS '99. Twelfth IEEE International Conference on , vol., no., pp.618-623, 17-21 Jan 1999

[2] T. Garvin and M. Norton, "Approximation Methods: Damped and Undamped Oscillators." Internet: http://www.siue.edu/~mnorton/mat-340.pdf, Dec. 10th, 2006 [July 26th, 2011]

[3] C. Acar and A. Shkel, MEMS Vibratory Gyroscopes – Structural Approaches to Improve Robustness, 1st ed., Springer: New York, 2009, pp.93-101.

[4] L. Dong, R. Leland, "The Adaptive Control System of A MEMS Gyroscope with Time-varying Rotation Rate", 2005 American Control Conference, June 2005, Portland, OR/USA